Comprehensive Analysis of *CLE* Polypeptide Signaling Gene Expression and Overexpression Activity in Arabidopsis[1][C][W][OA]

JiHyung Jun[2], Elisa Fiume[2], Adrienne H.K. Roeder, Ling Meng, Vijay K. Sharma[3], Karen S. Osmont[4], Catherine Baker[5], Chan Man Ha, Elliot M. Meyerowitz, Lewis J. Feldman, and Jennifer C. Fletcher*

Plant Gene Expression Center, United States Department of Agriculture-Agricultural Research Service/University of California, Berkeley, Albany, California 94710 (J.J., E.F., V.K.S., K.S.O., C.M.H., J.C.F.); Department of Plant and Microbial Biology, University of California, Berkeley, Berkeley, California 94720 (J.J., E.F., L.M., V.K.S., K.S.O., C.M.H., L.J.F., J.C.F.); and Division of Biology, California Institute of Technology, Pasadena, California 91125 (A.H.K.R., C.B., E.M.M.)

Intercellular signaling is essential for the coordination of growth and development in higher plants. Although hundreds of putative receptors have been identified in Arabidopsis (*Arabidopsis thaliana*), only a few families of extracellular signaling molecules have been discovered, and their biological roles are largely unknown. To expand our insight into the developmental processes potentially regulated by ligand-mediated signal transduction pathways, we undertook a systematic expression analysis of the members of the Arabidopsis *CLAVATA3/ESR-RELATED* (*CLE*) small signaling polypeptide family. Using reporter constructs, we show that the *CLE* genes have distinct and specific patterns of promoter activity. We find that each Arabidopsis tissue expresses at least one *CLE* gene, indicating that CLE-mediated signaling pathways are likely to play roles in many biological processes during the plant life cycle. Some *CLE* genes that are closely related in sequence have dissimilar expression profiles, yet in many tissues multiple *CLE* genes have overlapping patterns of promoter-driven reporter activity. This observation, plus the general absence of detectable morphological phenotypes in *cle* null mutants, suggest that a high degree of functional redundancy exists among *CLE* gene family members. Our work establishes a community resource of CLE-related biological materials and provides a platform for understanding and ultimately manipulating many different plant signaling systems.

Plant growth and survival are critically dependent on the communication of information between cells. Intercellular signaling pathways convey cell fate information, regulate cell division and differentiation processes, propagate and amplify specific signaling states, and coordinate tissue responses and functions. The importance of cell-to-cell communication is underscored by the classification of 10% of the Arabidopsis (*Arabidopsis thaliana*) proteome as playing roles in signal transduction (Arabidopsis Genome Initiative, 2000). Yet, whereas more than 400 Arabidopsis genes encode receptor-like kinases (Shiu and Bleecker, 2001) that presumably function as transmembrane sensors for extracellular signals, only a few families of putative signaling molecules have been identified.

The *CLE* genes encode small polypeptides (less than 15 kD) that share several structural features. Each possesses either an N-terminal signal peptide or membrane anchor sequence, a large variable domain, and a highly conserved 14-amino acid motif called the CLE domain near the C terminus (Cock and McCormick, 2001). Biochemical evidence indicates that the full-length CLAVATA3 (CLV3) polypeptide is proteolytically processed (Ni and Clark, 2006) to a mature active 12- or 13-amino acid arabinosylated glycopeptide consisting of the CLE domain (Kondo et al., 2006; Ohyama et al., 2009). Synthetic peptides corresponding to the CLE motif of other CLE family members also show biological activity in various bioassays (Fiers et al., 2005; Ito et al., 2006), suggesting that such

[1] This work was supported by the National Science Foundation (Arabidopsis 2010 grant no. MCB 0313546).

[2] These authors contributed equally to the article.

[3] Present address: Monsanto Company, 700 Chesterfield Parkway West, Chesterfield, MO 63017.

[4] Present address: Biology Department, University of Massachusetts, 611 North Pleasant Street, Amherst, MA 01003.

[5] Present address: Stanford University School of Medicine, 300 Pasteur Drive, Stanford, CA 94305.

* Corresponding author; e-mail jfletcher@berkeley.edu.

The author responsible for distribution of materials integral to the findings presented in this article in accordance with the policy described in the Instructions for Authors (www.plantphysiol.org) is: Jennifer C. Fletcher (jfletcher@berkeley.edu).

[C] Some figures in this article are displayed in color online but in black and white in the print edition.

[W] The online version of this article contains Web-only data.

[OA] Open Access articles can be viewed online without a subscription.

www.plantphysiol.org/cgi/doi/10.1104/pp.110.163683

peptides are likely to be the functional *CLE* gene products.

The biological functions of only a few *CLE* genes are known. *CLV3* is a founding member of the family and plays a key role in the intercellular communication of stem cell fate during Arabidopsis development. *CLV3* is specifically expressed in the stem cell population of shoot and floral meristems (Fletcher et al., 1999). Secreted into the extracellular space (Rojo et al., 2002), the CLV3 polypeptide is perceived by CLV1 (Clark et al., 1997; Ogawa et al., 2008) and other transmembrane receptors (Jeong et al., 1999; Müller et al., 2008) in the underlying cells. This signal transduction pathway is a core component of a negative feedback loop linking the stem cell reservoir and the underlying organizing center (Brand et al., 2000). Signaling through the CLV pathway restricts stem cell accumulation by limiting the expression domain of the *WUSCHEL RELATED HOMEOBOX* (*WOX*) family transcription factor gene *WUSCHEL* (Laux et al., 1996), which promotes stem cell activity and *CLV3* expression (Schoof et al., 2000).

CLE gene activity also controls stem cell homeostasis in the root meristem. *CLE40* transcripts are present at low levels in all Arabidopsis tissues (Hobe et al., 2003), but in roots, *CLE40* is specifically expressed in the stele and in differentiating columella cells of the protective root cap (Stahl et al., 2009). CLE40 activity emanating from the columella cells promotes distal root meristem differentiation by acting through the receptor kinase ARABIDOPSIS CRINKLY4 in a negative feedback loop that limits the expression domain of the *WUS*-related gene *WOX5* (Stahl et al., 2009). *WOX5* is present in the quiescent center and promotes columella stem cell fate in the distal domain of the root meristem. Thus, CLE/WOX-mediated signaling modules regulate Arabidopsis stem cell fate in both the shoot and the root apical meristems.

Overexpression studies have uncovered other developmental processes that respond to CLE peptide activity. A number of *CLE* genes when misexpressed in the root apical meristem gradually inhibit root meristem maintenance (Casamitjana-Martínez et al., 2003; Fiers et al., 2004, 2005; Ito et al., 2006; Meng et al., 2010) via a signaling pathway that appears to be distinct from the CLE40 pathway. Plants overexpressing *CLE19*, *CLE21*, or *CLE25* form miniature rosettes and inflorescences and display anthocyanin overproduction and developmental delays (Strabala et al., 2006). Overexpression of *CLE42* or *CLE44* results in bushy, dwarfed plants with delayed development and reduced apical dominance, whereas *CLE18* or *CLE26* overexpression leads to enhanced root elongation (Strabala et al., 2006). Simultaneous overexpression of *CLE6* and *CLE41* produces stunted, bushy plants with increased hypocotyl vascular cell proliferation, suggesting that CLE peptides can function synergistically (Whitford et al., 2008). These phenotypes indicate roles for CLE family members in regulating many different aspects of development. Yet, although many Arabidopsis *CLE* genes cause morphological phenotypes when overexpressed, others still remain to be evaluated by this type of study.

Results from overexpression studies as well as in vitro bioassays revealed that multiple CLE peptides have the capacity to generate the same morphological phenotypes. More than a dozen CLE peptides can activate the CLV3 signaling pathway when ectopically expressed in the shoot meristem (Ni and Clark, 2006; Strabala et al., 2006; Jun et al., 2008; Meng et al., 2010). Application of 19 different synthetic CLE peptides in root growth assays can arrest root meristem growth (Ito et al., 2006; Strabala et al., 2006; Whitford et al., 2008), whereas the application of CLE41, CLE42, CLE43, or CLE44 peptides leads to suppressed xylem differentiation (Ito et al., 2006; Whitford et al., 2008). The CLE family has been divided into two functional classes on this basis, with A-type CLE peptides (CLV3, CLE1–CLE27, and CLE40) being capable of inducing root and/or shoot meristematic cell differentiation, whereas B-type CLE peptides (CLE41–CLE44) are not (Whitford et al., 2008). These observations also raise the possibility that another key determinant of CLE peptide specificity, in addition to their primary amino acid sequence (Meng et al., 2010), may be their tissue distribution. Yet, although reverse transcription (RT)-PCR studies show that *CLE* genes are transcribed in many different tissues (Sharma et al., 2003), their specific expression patterns remain to be characterized.

To obtain a more precise understanding of the extent of overlap between *CLE* genes and gauge their possible functional redundancy, we used reporter assays to obtain high-resolution expression data for the entire Arabidopsis A-type *CLE* gene family. We observed highly specific *CLE* gene promoter activity patterns in roots, shoots, leaves, stems, and flowers, with most tissues expressing multiple *CLE* genes. We thus uncover a number of new biological processes that may be regulated by small-peptide signal transduction pathways. In addition, we characterized the overexpression phenotypes of previously unstudied *CLE* genes and identified hypomorphic or null insertion alleles for eight A-type *CLE* genes. Morphological examination of homozygous *cle* single mutant plants revealed no detectable growth or development phenotypes. Taken together, our expression and functional data indicate that *CLE* family members have diverse activities, yet significant functional redundancy exists among them.

RESULTS

Analysis of A-Type CLE Promoter Activity in Vegetative Tissues

Among the Arabidopsis A-type *CLE* genes, the expression patterns of *CLV3*, *CLE19*, and *CLE40* have already been reported (Fletcher et al., 1999; Hobe et al.,

2003; Fiers et al., 2004). To determine the expression patterns of the other A-type *CLE* genes, we generated *CLE* promoter:*GUS* or *GFP* fusion constructs using from 974 to 3,398 bp of the 5′ genomic region upstream of each *CLE* coding sequence. At least 10 independent transgenic lines were analyzed for each gene promoter to monitor consistent reporter activity, with the exception of the *CLE11*, *CLE12*, and *CLE13* promoters, for which four to eight independent transgenic lines were analyzed. Each *CLE* promoter drove GUS expression in one consistent pattern except for *CLE10* (Supplemental Materials and Methods S1). We observed that all but one A-type *CLE* gene reporter is expressed in vegetative tissues (Table I; Figs. 1–4).

Seedling Expression Patterns

We first analyzed *CLE* promoter activity in 11-d-old Arabidopsis seedlings (Fig. 1). From this analysis, the *CLE* expression patterns could be divided into three groups: (1) those expressed in both shoot and root tissue (15 genes); (2) those expressed only in shoot tissue (two genes); and (3) those expressed only in root tissue (five genes), as listed in Table I. *CLE8* was the only *CLE* gene for which expression was not detected at this stage of development.

Among the *CLE* genes with promoter activity in aerial tissues, *CLE12*, *CLE18*, *CLE22*, *CLE25*, and *CLE26* all display GUS activity in the vascular tissues (Fig. 1, A–E). Among these, *CLE12* staining is relatively weak in secondary and tertiary veins compared with primary veins and is stronger in the root than in the shoot (Figs. 1A and 2C). *CLE18* and *CLE22* are expressed uniformly in vascular tissue throughout the rosette leaves, although *CLE18* promoter activity begins later during leaf growth than *CLE22* (Fig. 1, B and C). The patterns of *CLE25* and *CLE26* promoter activity are complementary during leaf development. *CLE25* is strongly expressed in the vascular tissue of young leaf primordia but weaker in mature leaves (Figs. 1D and 2A). *CLE26* is initially detected in the leaf tip region where vein patterning initiates and only later expands into the vasculature throughout the entire leaf (Figs. 1E and 2B).

The *CLE9*, *CLE16*, *CLE17*, and *CLE27* promoters drive GUS activity in rosette leaf blade cells (Fig. 1, F–I). *CLE9* is expressed specifically in the stomatal developmental lineage, including meristemoid cells, guard mother cells, and young guard cells, throughout the aerial portions of the plant (Figs. 1F and 2, I and J). *CLE16* promoter activity is detected throughout the blade pavement cells, whereas *CLE17* and *CLE27* promoter activity is broad in young leaves but becomes predominantly marginal as the leaves mature. *CLE16* and *CLE17* promoter activities are also detected in the trichomes (Figs. 1, G and H, and 2, D and E), as is *CLE14* promoter activity (Supplemental Fig. S1, E and G). *CLE10* activity is restricted to the rosette leaf

Table I. *Summary of pCLE:GUS activity during vegetative development*

CLE Gene	Shoot					Root				
	Shoot Apex[a]	Hypocotyl	Vasculature	Leaf Blade	Other[b]	Tip[c]	Vasculature	Ground Tissues	Epidermis	Other[d]
CLE1						+	+	+		
CLE2										+
CLE3					+		+	+		
CLE4					+		+			
CLE5					+		+			+
CLE6					+					+
CLE7							+	+		
CLE8										
CLE9					+					
CLE10					+	±[e]				
CLE11		+			+	+				+
CLE12		+	+				+			
CLE13						+				
CLE14									+	+
CLE16	+	+		+	+	+	+		+	+
CLE17	+	+		+	+	+	+	+	+	+
CLE18			+			+	+			
CLE20							+			+
CLE21		+			+					
CLE22		+	+			+	+			
CLE25			+			+	+			
CLE26		+	+			+	+			
CLE27	+	+		+		+				+

[a]Shoot apex includes SAM and rosette leaf primordia. [b]Other includes pith, stipules, stomata, hydathodes, leaf margins, trichomes, and the leaf base. [c]Root tip includes root cap, root apical meristem, and cell division zone. [d]Other includes root hair cells and lateral root branch points. [e]Eight of 15 p*CLE10*:*GUS* lines showed root tip expression.

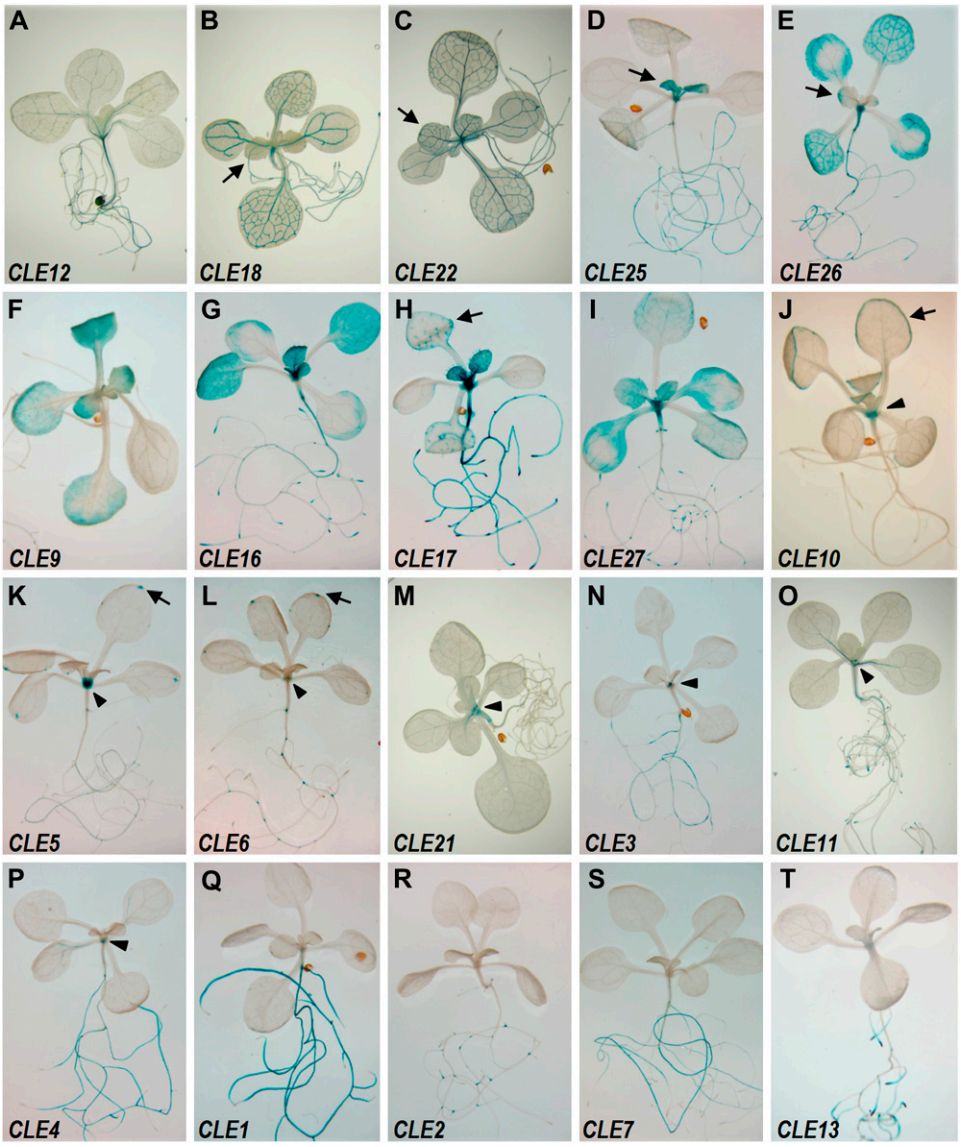

Figure 1. *CLE* promoter activity in 11-d-old-seedlings. A, *CLE12*. B, *CLE18*. C, *CLE22*. D, *CLE25*. E, *CLE26*. F, *CLE9*. G, *CLE16*. H, *CLE17*. I, *CLE27*. J, *CLE10*. K, *CLE5*. L, *CLE6*. M, *CLE21*. N, *CLE3*. O, *CLE11*. P, *CLE4*. Q, *CLE1*. R, *CLE2*. S, *CLE7*. T, *CLE13*. Arrows indicate GUS activity in the vasculature of young leaves (A–D), leaf margins (H and J), and hydathodes (K and L). Arrowheads (J–P) indicate GUS activity in the shoot apex.

margins (Fig. 1J), particularly in the hydathode region (Fig. 2H). The *CLE5* and *CLE6* promoters also drive specific GUS staining in the hydathode region (Figs. 1, K and L, and 2, F and G).

Other seedling tissues also express multiple *CLE* gene reporters. Hypocotyls display GUS activity driven by eight *CLE* promoters (Figs. 1, A, C, E, G, H, I, and M, and 2, L and M; Table I). The shoot apex region exhibits GUS activity driven by the *CLE3* to *-6*, *CLE10*, *CLE11*, *CLE16*, *CLE17*, *CLE21*, and *CLE27* promoters (Fig. 1, G–P). Among these, *CLE3* and *CLE11* show stipule-specific expression (Figs. 1, N and O, and 2, K and L). *CLE4* is limited to the pith region (Figs. 1P and 2Q), whereas *CLE5*, *CLE6*, *CLE10*, and *CLE21* expression is restricted to the base of the rosette leaves and is excluded from the shoot apical meristem (SAM; Figs. 1, J–M, and 2, M–P). *CLE16*, *CLE17*, and *CLE27* are expressed in initiating leaf primordia (see below). GUS activity driven by the *CLE1*, *CLE2*, *CLE7*, and *CLE13* promoters is specific to root tissue (Fig. 1, Q–T).

Root Expression Patterns

The promoters of many *CLE* genes are active in the root system of 11-d-old seedlings. GUS activity from four *CLE* promoters is detected throughout the primary root cap (Fig. 3, A–D). *CLE16* activity localizes to the root cap and the elongation zone but is absent from the meristematic division zone (Fig. 3E), whereas *CLE17* activity is absent from the root cap but localizes to the meristematic zone and the distal end of the elongation zone (Fig. 3F). *CLE22* activity is limited to a single file of newly differentiating vascular cells (Fig. 3G), whereas *CLE25* and *CLE26* activity is restricted to the vascular parenchyma (Fig. 3, H and I). Vascular tissue in the elongation zone exhibits GUS activity

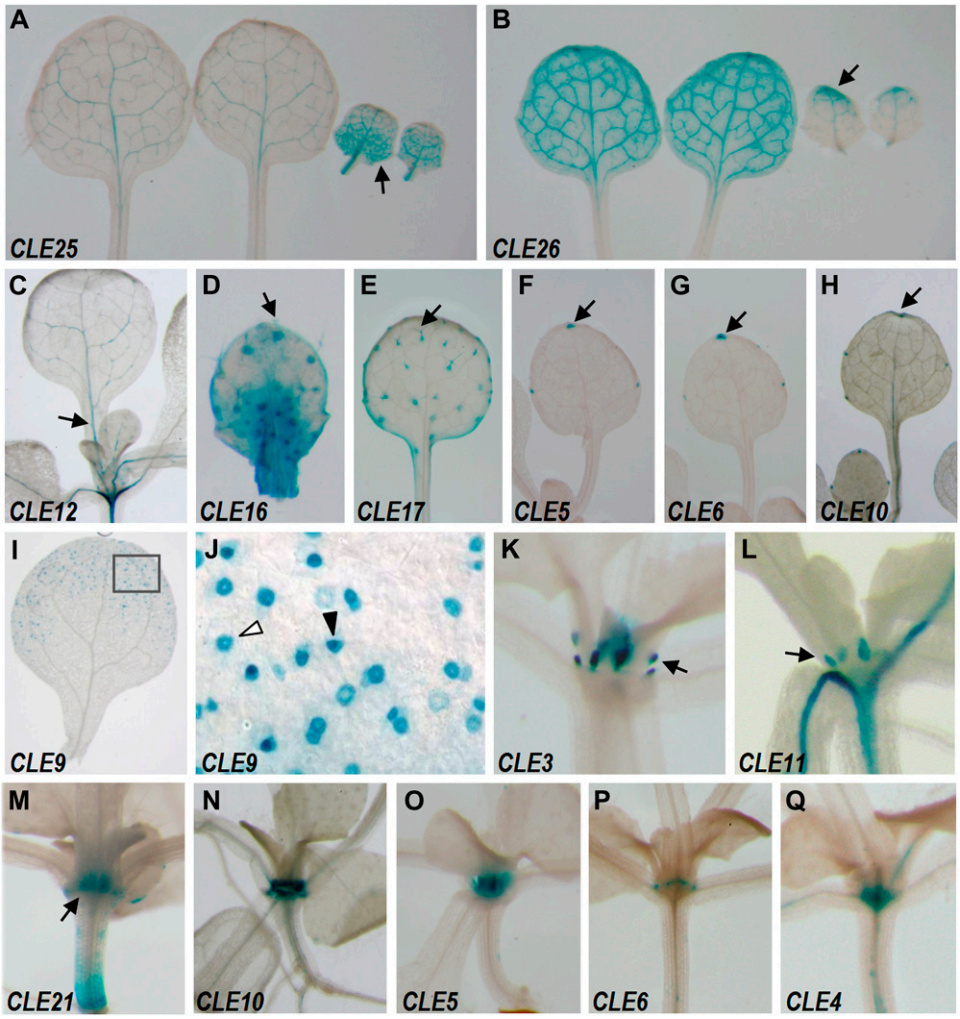

Figure 2. *CLE* promoter activity in 11-d-old-seedlings. A to C, *CLE25* (A), *CLE26* (B), and *CLE12* (C) in leaf vascular tissue. D, *CLE16* in trichomes and leaf blade. E, *CLE17* in trichomes and leaf margin. F to H, *CLE5* (F), *CLE6* (G), and *CLE10* (H) in hydathodes. I, *CLE9* in stomata. J, Magnified view of the region boxed in I. K to M, *CLE3* (K), *CLE11* (L), and *CLE21* (M) in stipules. N to P, *CLE10* (N), *CLE5* (O), and *CLE6* (P) in the leaf base. Q, *CLE4* in the pith. In A and B, first to fourth rosette leaves are arranged in order from the left. Arrows indicate GUS activity in the vasculature of the basal and apical regions of young leaves (A and B, respectively) and in the midvein (C), trichomes (D and E), hydathodes (F–H), and stipules (K–M). Black and white arrowheads in J indicate a meristemoid cell and a young guard cell, respectively.

from both the *CLE1* and *CLE18* promoters (Fig. 3, A and D).

More mature root tissues express multiple *CLE* gene reporters in overlapping patterns. We examined two different areas of 11-d-old primary and lateral roots: a younger region with immature hair cells as well as an older region with fully differentiated hair cells. We found that the stele in both areas of the root exhibits GUS activity driven by five different *CLE* promoters (Fig. 4, A–H; Table I). p*CLE20*:*CLE20-GFP* fusion protein activity is observed in the protoxylem and metaxylem (Supplemental Fig. S1B), whereas *CLE25* and *CLE26* promoter activity is restricted to the metaxylem (Supplemental Fig. S2A; data not shown). *CLE22* is strongly detected in the vascular parenchyma (Supplemental Fig. S2B). Pericycle cells specifically display GUS activity from the *CLE4* and *CLE18* promoters (Fig. 4, I–L; Supplemental Fig. S2C), whereas both the pericycle and endodermis express *CLE7* (Fig. 4, M and N; Supplemental Fig. S2D). *CLE1* promoter activity is detected throughout the endodermis and the stele (Fig. 4, O and P; Supplemental Fig. S2E). In contrast, p*CLE14*:*GFP* activity is restricted to the root epidermis (Supplemental Fig. S1F).

Several *CLE* promoters are active in a spatially and temporally restricted fashion in the primary root. In the less mature region of the root, p*CLE16*:*GUS* and p*CLE17*:*GUS* activity are found exclusively in the epidermis (Fig. 4, Q and S), whereas in the older region, *CLE16* promoter activity localizes to the stele (Fig. 4R) and *CLE17* promoter activity expands throughout the root (Fig. 4T). *CLE3* promoter activity is patchy in the stele in the less mature root region (Fig. 4U) but becomes limited to the pericycle and endodermis in older tissue (Fig. 4V). Finally, *CLE5* promoter activity is not detected until the primary root is fully differentiated, when very weak activity is observed in the stele (Fig. 4, W and X).

CLE promoter activity is highly dynamic during lateral root formation. *CLE27* promoter-driven GUS activity is detected in the cortex of the primary root at lateral root inception (Supplemental Fig. S3A). As the lateral root cells begin to grow out, the *CLE27* reporter is expressed throughout the dome but most strongly in

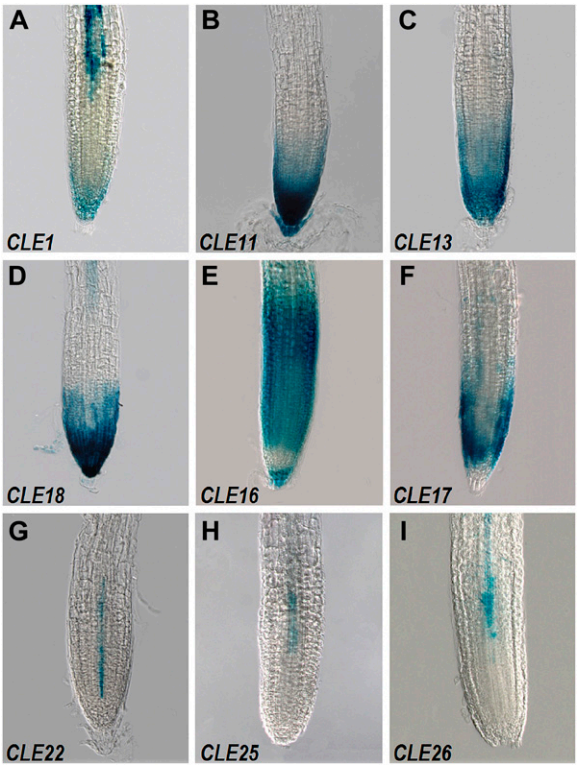

Figure 3. *CLE* promoter activity in the primary root tips of 11-d-old-seedlings. A, *CLE1* in the root cap and vascular parenchyma. B to D, *CLE11* (B), *CLE13* (C), and *CLE18* (D) in the root cap and apical meristem. E, *CLE16* in the root cap and throughout the elongation zone. F, *CLE17* in the root apical meristem. G, *CLE22* in the newly differentiating vascular tissue. H and I, *CLE25* (H) and *CLE26* (I) in the vascular parenchyma.

a ring around the base (Supplemental Fig. S3, B and C). As outgrowth continues, *CLE27* promoter activity is lost from the lateral root tip but remains detectable in the more basal region (Supplemental Fig. S3, D and E). In mature lateral roots, *CLE27* promoter activity is found at the base of the lateral root where it joins the primary root (Supplemental Fig. S3F) as well as in the meristematic zone (Supplemental Fig. S3G). *CLE2* and *CLE20* reporter expression is likewise detected at the base of initiating lateral roots (Supplemental Figs. S1, C and D, and S3, H and I), although at a slightly later stage than *CLE27*. As root outgrowth progresses, *CLE2* promoter activity becomes confined to the interior cells at the junction between the primary and lateral roots (Supplemental Fig. S3J). Similarly, *CLE11* promoter-driven GUS activity is observed in a small group of cells surrounding the initiating lateral roots (Supplemental Fig. S3K) as well as at the root tip and is sustained at the junction between the primary and lateral roots (Supplemental Fig. S3L). *CLE5* and *CLE6* promoter activity is also seen specifically in the interior cells at the junction between the primary root and the mature lateral roots (Supplemental Fig. S3, M and N).

CLE promoter activity is also dynamic in the lateral root vasculature. *CLE22* is expressed earliest during lateral root formation (Supplemental Fig. S3, O and P), followed by *CLE25* (Supplemental Fig. S3Q). p*CLE25*:*GUS* and p*CLE26*:*GUS* activity both localize to the vasculature of outgrowing lateral roots (Supplemental Fig. S3, Q and R), whereas *CLE4* (Supplemental Fig. S3S) and *CLE12* (Supplemental Fig. S3T) activity is restricted to the mature lateral root vasculature. *CLE7* promoter-driven activity is likewise limited to the mature lateral root vasculature, but unlike the others, its expression is absent from the junction between the primary and lateral roots (Supplemental Fig. S3U). Thus, the expression of half a dozen *CLE* reporters is induced at various stages during the development of the lateral root vasculature.

Lateral root tips initiate the expression of different *CLE* reporters at various stages during their formation. GUS activity driven by the promoters of both *CLE16* and *CLE17* is detected throughout the initiating lateral roots, before becoming confined to the tips and meristematic zones as the roots grow out (Supplemental Fig. S4, A–H). *CLE11* (Supplemental Fig. S4I) and *CLE13* (Supplemental Fig. S4K) activity initiates at the lateral root tip at a slightly later point during outgrowth, followed by *CLE18* promoter activity (Supplemental Fig. S4M) and *CLE1* activity (Supplemental Fig. S4O). The promoters of all six of these *CLE* genes are active in the root caps of mature lateral roots (Supplemental Fig. S4, D, H, J, L, N, and P). Yet, unlike the other five, which are localized in all root cap cells, *CLE1* promoter activity in lateral roots is restricted to the interior layers of the root cap. *CLE18* reporter signal is strong in the root cap and weaker in cells at the very distal end of the elongation zone. In addition, initiating vascular tissues display *CLE22* promoter activity (Supplemental Fig. S4Q) and more mature vascular tissues display *CLE25* and *CLE26* promoter activity (Supplemental Fig. S4, R and S). Lateral roots, therefore, express different combinations of *CLE* gene reporters in overlapping patterns throughout their development.

Eight *CLE* genes are represented on the ATH1 microarray used to generate a spatiotemporal map of gene expression in the roots of 5- to 7-d-old seedlings (Brady et al., 2007). Comparison of our results with this data set using the eFP Browser (Cartwright et al., 2009) showed congruent profiles for *CLE3*, *CLE12*, and *CLE17*. However, we did not detect activity of *CLE2* in the phloem, *CLE6* in phloem companion cells, *CLE21* in epidermal cells of the elongation region, or *CLE27* in primary root cortex and lateral root cap cells (Brady et al., 2007). Furthermore, *CLE26* is reported in the metaphloem, whereas we detect it in the metaxylem. These discrepancies likely reflect the increased sensitivity of transcriptional profiling compared with GUS reporter analysis, the use of insufficient *CLE* regulatory sequence for some reporter constructs, and/or the difference in developmental age between the samples evaluated.

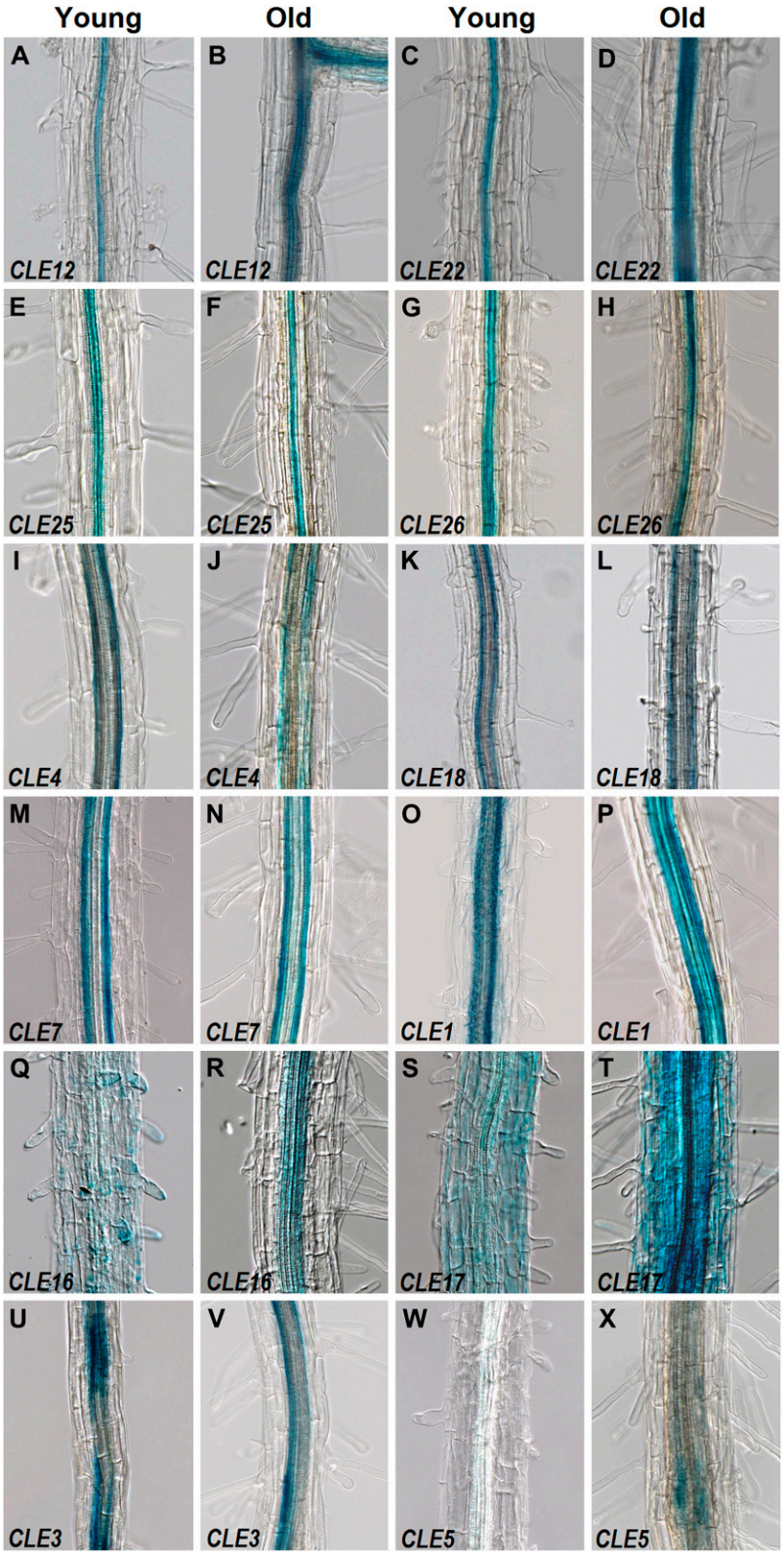

Figure 4. *CLE* promoter activity in primary root cell files. A to H, *CLE12* (A and B), *CLE22* (C and D), *CLE25* (E and F), and *CLE26* (G and H) in the stele. I to L, *CLE4* (I and J) and *CLE18* (K and L) in the pericycle. M to O, *CLE7* (M and N) and *CLE1* (O) in the pericycle and endodermis. P, *CLE1* in the stele and endodermis. Q, *CLE16* in the epidermis. R, *CLE16* in the stele. S, *CLE17* in the epidermis. T, *CLE17* throughout the root. U to X, *CLE3* (U and V) and *CLE5* (W and X) in patches around the vascular bundle. Images in A, C, E, G, I, K, M, O, Q, S, U, and W were taken from regions of 11-d-old primary or lateral roots where the root hair cells are not fully mature. Images in B, D, F, H, J, L, N, P, R, T, V, and X were taken from the primary root maturation zone with fully differentiated root hair cells.

Analysis of A-Type CLE Promoter Activity in Reproductive Tissues

With a few exceptions, such as those for *CLE2* and *CLE8*, most A-type *CLE* gene reporters are expressed during reproductive growth (Table II; Figs. 5–7). As in seedlings, each reproductive tissue expresses more than one *CLE* gene reporter. Conversely, most *CLE* gene reporters are expressed in more than one repro-

Table II. *Summary of pCLE:GUS activity during reproductive development*

CLE Gene	Stem/ Pedicels	Branching Points	Cauline Leaves	Sepals/ Petals	Stamens		Gynoecium				Flower Base[a]
					Anthers	Filament	Stigma	Style	Ovary[b]	Ovules	
CLE1					+			+			
CLE2											
CLE3			+								
CLE4		+				+					+[c]
CLE5		+						+			+
CLE6		+				+					+
CLE7					+						
CLE8											
CLE9	+		+	+[d]							
CLE10		+	+				+	+	+	+	
CLE11					+			+			
CLE12	+[e]		+		+						+
CLE13	+[e]				+						+
CLE14				+[d]							
CLE16	+			+[e]		+			+		+
CLE17	+	+	+	+			+	+	+[c]		
CLE18			+	+[d,e]		+					
CLE20	+[e]										
CLE21		+							+		+
CLE22	+[e]		+	+[e]					+[e]		+
CLE25	+[e]				+				+[e]	+	
CLE26	+[e]		+	+[d,e]		+			+[e]		+
CLE27		+								+	+

[a]Includes receptacle and abscission zone. [b]Includes valves, replum, and septum. [c]Siliques only. [d]Sepals only. [e]Vasculature.

ductive tissue, yet their individual expression patterns are highly specific and restricted.

Inflorescence Expression Patterns

The promoters of many *CLE* genes are active in inflorescence tissues. GUS activity from the *CLE16* promoter is found specifically in the epidermis (Fig. 5A). The *CLE12*, *CLE13*, *CLE20*, *CLE22*, *CLE25*, and *CLE26* reporters are expressed in the stem vasculature (Fig. 5, B–F; data not shown), in each case more strongly in the primary inflorescence branching points than elsewhere in the stem. Activity from seven *CLE* promoters is largely restricted to the primary branching points of the stem (Fig. 5, G–M; Table II), although *CLE17* promoter activity is also present in the stem trichomes. Consistent with its expression in vegetative tissues, signal from the *CLE9* reporter is detected in the stomata of stem epidermal cells (Fig. 5N). Pedicels display promoter-driven GUS activity from *CLE16* in the epidermis (Fig. 5P), from *CLE22* and *CLE26* in the vasculature (Fig. 5, Q and R), and from *CLE27* throughout (Fig. 5S).

Eight *CLE* promoters are active in the cauline leaves. *CLE12* and *CLE22* promoter activity is strong in the proximal vasculature and at the very tip of the cauline leaf (Fig. 5, B and D). The *CLE26* promoter drives patchy vascular expression in the blade (Fig. 5F). *CLE18*-driven expression is detected in the vasculature and at the leaf margins (Fig. 5O), whereas *CLE10* and *CLE17* promoter-driven GUS activity is limited to the leaf margins (Fig. 5, J and K). *CLE9* expression is only detected in stomatal cells (Fig. 5N), and *CLE3* expression is restricted to stipules (data not shown). Promoter activity from all eight genes is also detected in rosette leaves.

Flower Expression Patterns

Floral tissues display highly complex *CLE* promoter activity patterns (Fig. 6). Sepals and petals express nine different *CLE* gene reporters. *CLE9* promoter activity is detected in the sepal stomatal cells, consistent with what is observed in vegetative tissues (Fig. 2J). The *CLE14* reporter is expressed in sepal trichomes (Supplemental Fig. S1H). *CLE16* promoter activity is detected in sepal and petal vasculature throughout flower development, although it is stronger at the distal ends in young flowers (Fig. 6A) and becomes confined to these regions in fully mature flowers (Fig. 6H). *CLE18* and *CLE26* reporters are expressed in sepal veins, more strongly in their distal portion (Fig. 6, B and C). *CLE22* promoter activity is observed uniformly in the vasculature of both sepals and petals, although it becomes more pronounced in the sepal veins in fully developed flowers (Fig. 6D). *CLE17* promoter activity is detected along the margins of sepals and petals in young flower buds (Fig. 6E). *CLE5* and *CLE6* reporters are expressed at the base of each flower organ type, above the abscission zone (Fig. 6, F and G).

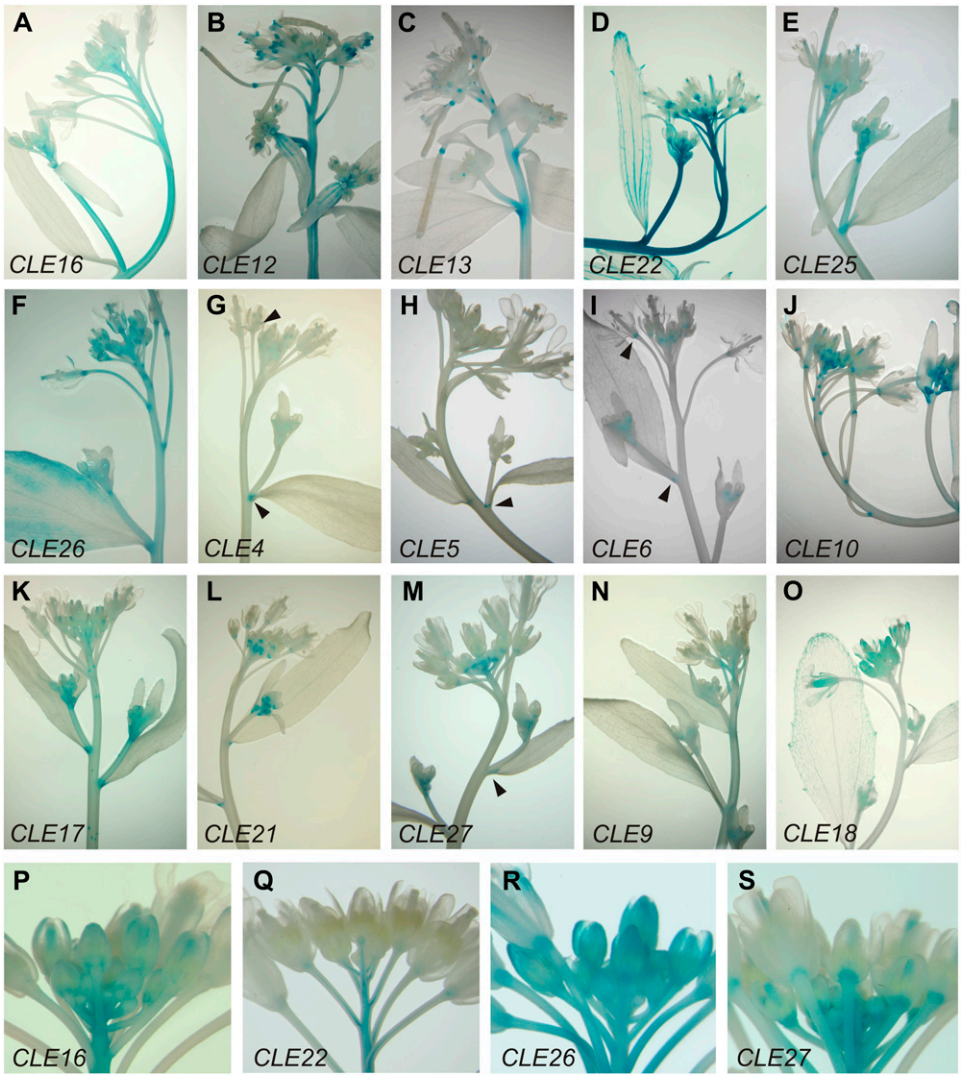

Figure 5. *CLE* promoter activity in inflorescences and cauline leaves. A, *CLE16* in the epidermis. B to F, *CLE12* (B), *CLE13* (C), *CLE22* (D), *CLE25* (E), and *CLE26* (F) in the vasculature. The *CLE22* stem is overstained to visualize GUS activity in the cauline leaf. G to M, *CLE4* (G), *CLE5* (H), *CLE6* (I), *CLE10* (J), *CLE17* (K), *CLE21* (L), and *CLE27* (M) in the inflorescence branching points. N, *CLE9* in the stomata. O, *CLE18* in the cauline leaf vasculature and marginal cells. P, *CLE16* in the epidermis. Q and R, *CLE22* (Q) and *CLE26* (R) in the vasculature. S, *CLE27* throughout the pedicels.

The male reproductive structures express a variety of *CLE* gene reporters (Fig. 6). Each stamen-expressed reporter is present in either the anther or the filament but not in both. Five *CLE* reporters are expressed in the filament (Table II). *CLE16* and *CLE18* are uniformly detected throughout the entire filament (Fig. 6, H and I). In contrast, *CLE6* promoter activity is detected very weakly in the distal region of the filament (Fig. 6G), whereas *CLE4* and *CLE26* promoter activity is limited to the distal tip of the filament, where it connects to the anther (Fig. 6, J and K). *CLE4* is the only one of these that is expressed exclusively in the filament and not in other floral tissues.

Anthers express six different *CLE* gene reporters (Table II). *CLE1* promoter activity is found in both pollen grains and tapetum cells of anthers from their emergence in stage 6 floral buds until maturation (Fig. 6L). The *CLE25* reporter is expressed throughout the anthers in young developing flowers (Fig. 6M). In mature flowers, *CLE25* expression become more restricted and overlaps with that of *CLE7* in the central region of the anther sacs, along the boundaries with the connective tissue (Fig. 6N). *CLE11*, *CLE12*, and *CLE13* promoter activity is evident solely in pollen grains. The *CLE12* reporter is expressed throughout all stages of pollen development (Fig. 6O). However, *CLE11* and *CLE13* reporters show a dynamic and complementary expression pattern: the *CLE11* reporter is expressed only in fully mature pollen grains (Fig. 6, P and Q), whereas the *CLE13* reporter is expressed only in young developing anthers (Fig. 6, R and S).

The female reproductive structure exhibits *CLE* promoter activity in a variety of complex patterns (Fig. 7). The *CLE10* reporter is the most broadly expressed, its activity being detected in the stigma, style, transmitting tract, septum, and ovules (Fig. 7A). The style also displays promoter activity from *CLE1*, *CLE5*, and *CLE11*. Among these, *CLE5* and *CLE1* reporters are expressed in the transmitting tract of the style (Fig. 7, B and C), whereas *CLE11* reporter expression is observed in a central region that appears to correspond to the transmitting tract or vascular fans

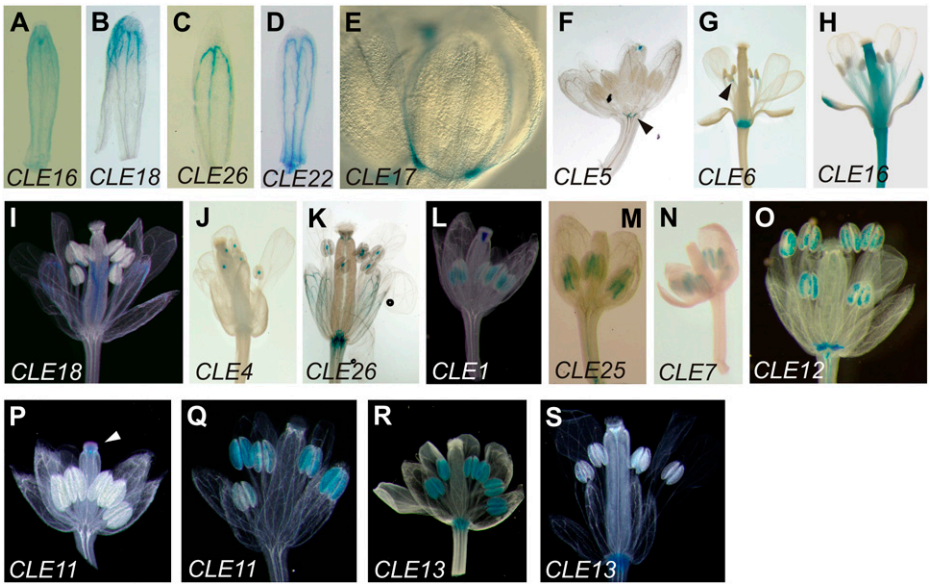

Figure 6. *CLE* promoter activity in flowers. A to D, *CLE16* (A), *CLE18* (B), *CLE26* (C), and *CLE22* (D) in sepal vasculature. E, *CLE17* in sepal and petal margins. F and G, *CLE5* (F) and *CLE6* (G) at the base of the flower. H to K, *CLE16* (H), *CLE18* (I), *CLE4* (J), and *CLE26* (K) in the stamen filaments. L to N, *CLE1* (L), *CLE25* (M), and *CLE7* (N) in the anthers. O to S, *CLE12* (O), *CLE11* (P and Q), and *CLE13* (R and S) in the pollen grains.

(Fig. 7D). Uniquely, *CLE17* promoter activity is detected in a ring at the margin between the stigmatic tissue and the style, in the transmitting tract, and in the septum (Fig. 7E). *CLE21* promoter activity is observed in the valve margins (Fig. 7F), whereas *CLE16* promoter activity occurs in the valves (Fig. 7G). The vasculature of the gynoecium exhibits *CLE22*, *CLE25*, and *CLE26* promoter activity (Fig. 7, H–J). *CLE25* reporter expression is additionally detected in the septum, funiculi, and at the proximal end of the ovules (Fig. 7K), whereas the *CLE27* reporter is expressed throughout the funiculi and ovules of fully mature flowers (Fig. 7L). Finally, the abscission zone exhibits promoter activity from *CLE10* (Fig. 5J), *CLE12* (Fig. 6O), *CLE13* (Fig. 6, R and S), *CLE16* (Fig. 6H), *CLE21* (Fig. 7F), *CLE22* (Fig. 7H), *CLE26* (Fig. 7J), and *CLE27* (Fig. 7M). These promoter activity patterns are consistent throughout gynoecium and silique development, with two exceptions. First, *CLE17* reporter expression shifts from the stigma/style region in carpels to the

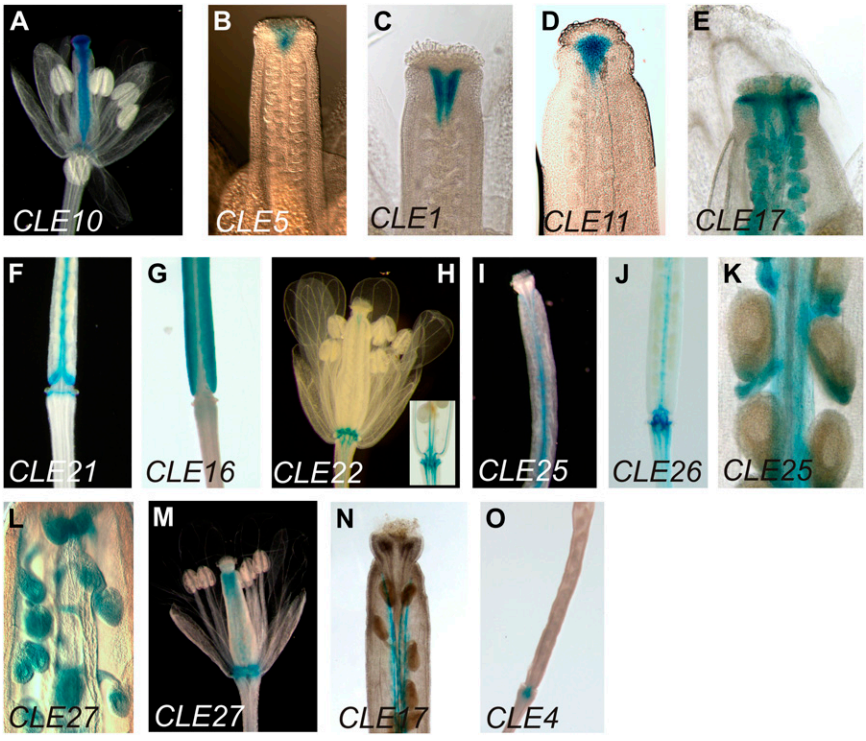

Figure 7. *CLE* promoter activity in the gynoecium. A, *CLE10* in the stigma, style, and central tissues. B to D, *CLE5* (B), *CLE1* (C), and *CLE11* (D) in the style. E, *CLE17* at the stigma/style boundary. F, *CLE21* in the valve margins. G, *CLE16* in the valves. H to J, *CLE22* (H), *CLE25* (I), and *CLE26* (J) in the vasculature. The inset in H shows *CLE22* in the basal vasculature and abscission zone. K, *CLE25* in the funiculi and ovules. L and M, *CLE27* in the ovules (L) and abscission zone (M). N, *CLE17* in the silique valve margins. O, *CLE4* in the silique receptacle.

valve margins in siliques (Fig. 7N). Second, *CLE4* reporter expression becomes detectable specifically in the silique receptacle (Fig. 7O). In sum, our observations indicate that different *CLE* promoters drive GUS activity in complex, overlapping spatial and temporal patterns, particularly in the reproductive tissues.

Detailed Analysis of CLE Promoter Activity in Shoot Apices

Promoter activity from 10 different *CLE* genes is detected around the shoot apex region of seedlings (Figs. 1 and 2). We examined their expression patterns in greater detail by sectioning 10-d-old GUS-stained seedlings. We found that *CLE21* promoter activity is restricted to the stipules (Supplemental Fig. S5A), whereas *CLE10* promoter activity is detected in stipules and in a proximal, adaxial domain of leaf primordia (Supplemental Fig. S5B). *CLE4* and *CLE26* promoter activity is located in the pith and the ground cells of the hypocotyl, respectively (Supplemental Fig. S5, C and D).

In contrast, the *CLE16*, *CLE17*, and *CLE27* reporter constructs show consistent activity in or adjacent to the SAM in multiple independent transgenic lines. Compared with untransformed wild-type plants (Fig. $8A_1$) and p*CLV3*:*GUS* plants (Fig. $8B_1$), *CLE16* promoter activity is detected throughout initiating leaf primordia on the SAM flanks (Fig. $8C_1$). As the leaf primordia develop, *CLE16* GUS activity is stronger in the proximal than the distal region and in the L1 cells (Fig. $8C_1$; Supplemental Fig. S6, A and B). A similar pattern is observed in p*CLE17*:*GUS* leaf primordia (Fig. $8D_1$). However, *CLE17* promoter activity is also detected in the SAM (Fig. $8D_1$). Transgenic plants with weak *CLE17* promoter activity show GUS staining in the outer layers of the central zone and the peripheral zone (PZ; Supplemental Fig. S6C). Transgenic plants with strong *CLE17* promoter activity exhibit GUS staining throughout the SAM and initiating leaf primordia, most strongly in the PZ and the outer cell layers (Supplemental Fig. S6D). *CLE27* promoter activity is exclusively detected in the epidermal layer of developing leaf primordia and young rosette leaves

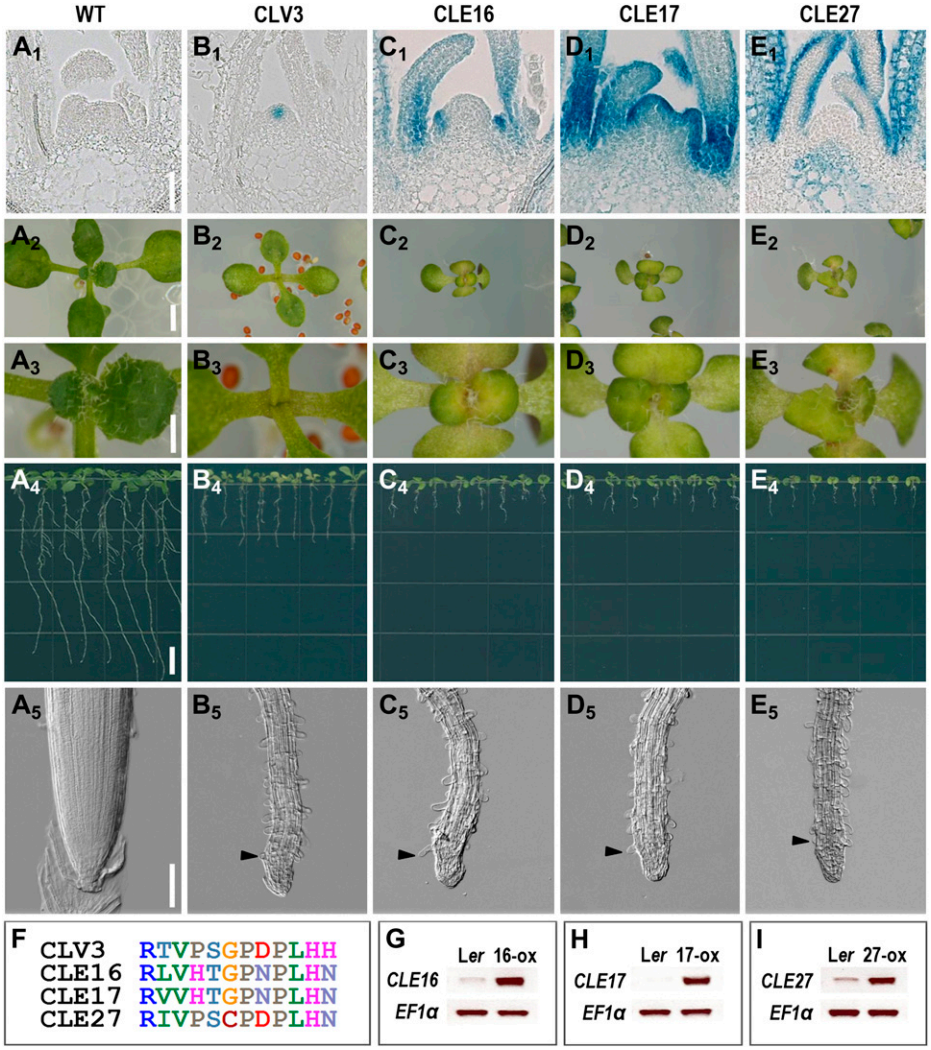

Figure 8. *CLE16*, *CLE17*, and *CLE27* overexpression phenotypes. A_1 to E_1, Longitudinal sections of 10-d-old wild-type (WT), p*CLV3*:*GUS*, p*CLE16*:*GUS*, p*CLE17*:*GUS*, and p*CLE27*:*GUS* plant shoot apices, respectively. A_2 to A_5, Thirteen-day-old Landsberg *erecta* (L*er*) seedlings. B_2 to B_5, Thirteen-day-old p*35S*:*CLV3* seedlings. C_2 to C_5, Thirteen-day-old p*35S*:*CLE16* seedlings. D_2 to D_5, Thirteen-day-old p*35S*:*CLE17* seedlings. E_2 to E_5, Thirteen-day-old p*35S*:*CLE27* seedlings. F, Comparison of CLE peptide sequences. Alignment was performed using MUSCLE (Edgar, 2004). Each color represents a different amino acid residue. G to I, RT-PCR analysis of *CLE* expression in transgenic plants. *EF1α* is used as a control. A_3 to E_3 are magnified views of shoot apex in A_2 to E_2. Nomarski images of the roots in A_5 to E_5 show root hair differentiation (arrowheads) close to the root tip. Bars = 100 μm in A_1 to E_1 and A_5 to E_5, 2.5 mm in A_2 to E_2, 1 mm in A_3 to E_3, and 5 mm in A_4 to E_4.

and in the pith region beneath the rib meristem (Fig. 8E_1; Supplemental Fig. S6, E and F). However, *CLE27* reporter expression is excluded from the SAM and the initiating leaf primordia on the meristem flanks. These results are consistent with Arabidopsis SAM transcription profiling data showing that *CLE27* mRNA is absent from the SAM but that *CLE17* is expressed at low levels in the central zone and organizing center and at moderate levels in the PZ (Yadav et al., 2009). *CLE16* is not represented in the profiling data set.

Because *CLE17* reporter expression in the SAM overlapped with the *CLV3* expression domain, we tested whether *CLE17* could activate the *CLV* signaling pathway by analyzing the phenotypes of p*35S*:*CLE17* transgenic plants. Ectopic expression of *CLV3* causes SAM arrest early during vegetative development (Fig. 8, B_2 and B_3) as well as premature floral meristem termination (Brand et al., 2000). In contrast, ectopic expression of *CLE17* does not confer a SAM termination phenotype (Fig. 8, D_2 and D_3), nor is floral organ formation affected. These data indicate that CLE17 cannot activate the CLV3 signaling pathway in either shoot or floral meristems. Instead, the rosette leaves of *CLE17*-overexpressing plants show a delayed growth rate and smaller and epinastic morphology compared with wild-type rosette leaves (Fig. 8, D_2 and D_3). Developmental timing is also delayed, and apical dominance appears to be reduced. In addition, *CLE17* overexpression (Fig. 8H) causes root apical meristem termination (Fig. 8, D_4 and D_5), as has been observed in plants that have been treated with exogenous CLE peptides or that overexpress other *CLE* genes, such as *CLV3* (Fig. 8, B_4 and B_5). Transgenic plants overexpressing either *CLE16* or *CLE27* (Fig. 8, G and I) display phenotypes that closely resemble those of p*35S*:*CLE17* plants (Fig. 8, C_2–C_5 and E_2–E_5).

Alignment of the CLE16, CLE17, and CLE27 peptides with that of CLV3 reveals altered amino acids at key residues in the CLE domain. Compared with CLV3, all three peptides contain an Asn instead of a His at position 12, CLE16 and CLE17 contain a His instead of a Pro at position 4 as well as an Asn instead of an Asp at position 8, and CLE27 contains a Cys instead of the highly conserved Gly at position 6 (Fig. 8F). These observations suggest that the failure of these three proteins to activate the CLV3 signaling pathway when overexpressed in the SAM may be due to differences in the composition of their CLE motifs.

CLE Overexpression Phenotypes in Shoots and Roots

Despite extensive overexpression studies that uncovered other developmental processes responding to CLE peptide activity, the overexpression phenotypes of a few *CLE* genes remain undetermined. To fill in this gap, we generated transgenic plants expressing the coding region of *CLE8*, *CLE12*, or *CLE22* under the control of the cauliflower mosaic virus 35S promoter and scored them for shoot and root meristem arrest phenotypes (Supplemental Table S1). We found that p*35S*:*CLE8* plants showed neither shoot nor root meristem defects (Supplemental Fig. S7B), whereas both p*35S*:*CLE12* and p*35S*:*CLE22* plants displayed SAM termination (Supplemental Fig. S7, C and D). Reduced root growth and root apical meristem arrest were also observed in *CLE12*- and *CLE22*-overexpressing plants (Supplemental Fig. S7, E and F). Our data are consistent with previous work except in the case of *CLE8*, which has been reported to trigger root apical meristem consumption when overexpressed (Ito et al., 2006). Combined with earlier studies, our results indicate that 16 of 26 A-type *CLE* genes, including *CLV3*, can induce SAM termination when overexpressed and that 18 (or 19) A-type *CLE* genes can induce root apical meristem termination.

Mutational Analysis of A-Type CLE Loci

To begin to determine the functions of additional A-type *CLE* genes, we obtained *cle* T-DNA insertion alleles from the publicly available collections. We identified one allele each with an insertion within the *CLE1*, *CLE10*, *CLE16*, and *CLE18* coding regions, one allele each with an insertion in the *CLE3*, *CLE7*, *CLE13*, and *CLE19* 5′ untranslated regions, and one allele with an insertion in the *CLE17* 3′ untranslated region (Fig. 9). We performed RT-PCR to examine *CLE* mRNA transcript levels in plants homozygous for each of these *cle* alleles. No transcripts were detected in *cle1-1*, *cle7-1*, *cle16-1*, and *cle18-1* plants (Fig. 9, A–D), indicating that they represent null alleles. Reduced transcript levels were detected in *cle3-1*, *cle10-1*, *cle13-1*, *cle17-1*, and *cle19-1* plants (Fig. 9, E–I), showing that these are hypomorphic alleles. For *cle3-1*, we observed a minor but reproducible decrease in *CLE3* mRNA levels (Fig. 9E). In addition, we identified T-DNA insertion alleles within 700 bp upstream or downstream of the *CLE2*, *CLE4*, *CLE6*, *CLE9*, *CLE17*, and *CLE21* coding regions, but RT-PCR experiments detected no significant reduction in transcript levels (Supplemental Table S2). Detailed inspection of seedling, inflorescence, flower, and root development revealed no detectable morphological defects in plants homozygous for any of these *cle* alleles, suggesting that substantial functional redundancy occurs among A-type *CLE* family members.

DISCUSSION

Dozens of potential intercellular signaling molecules as well as hundreds of putative receptors have been cataloged in the Arabidopsis genome, yet relatively little is known about their individual expression patterns or functions. Several members of the A-type CLE family of small secreted polypeptides act to maintain cell fate in shoot and root apical meristems; however, the dearth of mutations in the other small *CLE* coding sequences has limited our insight into their biological activities. In addition, only a single

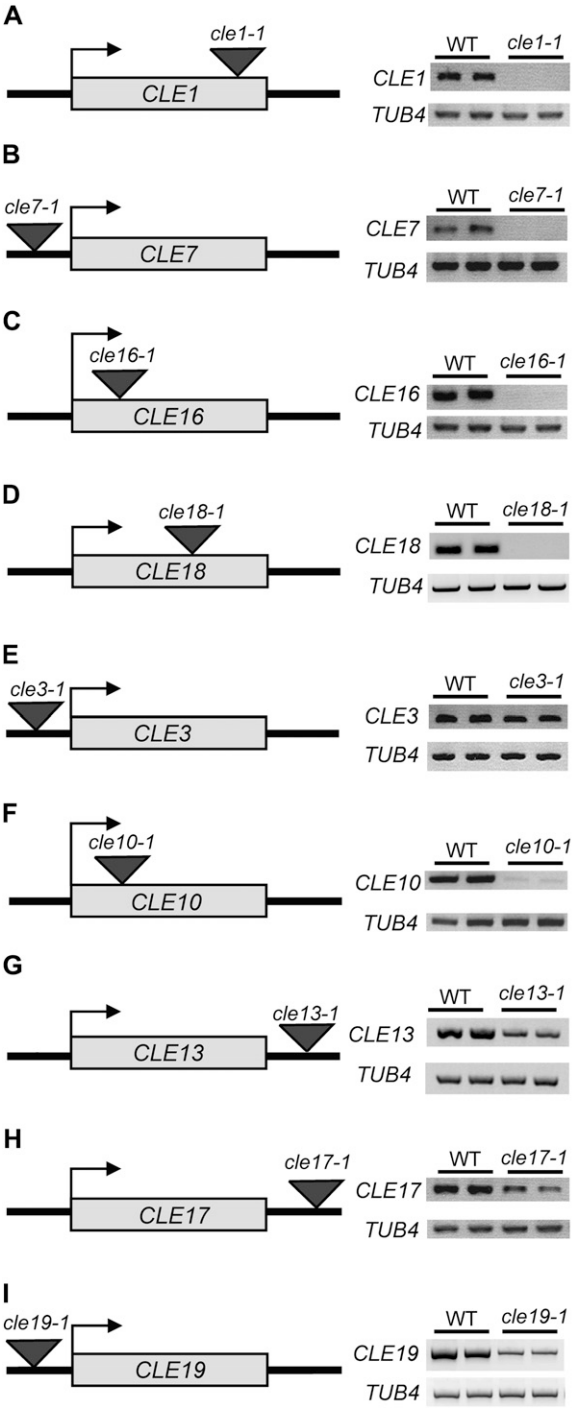

Figure 9. Characterization of *CLE* insertion alleles. Location of the insertion allele relative to each *CLE* coding region (gray box) and *CLE* mRNA transcript levels in two individual wild-type (WT) and homozygous *cle* mutant plants are shown. *TUBULIN4* (*TUB4*) was used as a control.

study of A-type *CLE* mRNA transcription profiles exists (Sharma et al., 2003), and few *CLE* genes are represented on microarrays, another source of detailed expression data. To address these deficiencies, we performed a comprehensive characterization of A-type *CLE* promoter expression during Arabidopsis vegetative and reproductive development and identified null or hypomorphic alleles of seven *CLE* genes.

One important finding from our work is that most Arabidopsis tissues express one or more *CLE* gene reporters (Fig. 10). This includes highly specialized cell types such as stomata, trichomes, and stipules. Primary roots display *CLE* promoter-driven expression in the root cap, the root apical meristem, and each radial cell layer (Figs. 3 and 4), and lateral root formation is associated with the dynamic activity of multiple *CLE* promoters (Supplemental Fig. S3). The vasculature is characterized by the expression of 14 *CLE* reporters, half of which are specific to either the root or the shoot vasculature. Multiple *CLE* gene reporters also are expressed in different tissues of the inflorescence stem (Fig. 5) as well as in each floral organ. In particular, the reproductive organs express a variety of *CLE* gene reporters in specific spatial and temporal patterns (Figs. 6 and 7). Seven different *CLE* reporters are expressed at the base of the flower, where the cognate genes may be involved in the signaling process(es) that controls floral organ abscission. These observations indicate that, beyond their functions in shoot and root apical meristems, CLE-mediated signal transduction pathways are likely to play roles in a wide variety of different biological processes.

Another intriguing finding is that the A-type *CLE* gene promoters drive highly distinct and specific patterns of expression. For example, the promoters of *CLE3*, *CLE5*, *CLE16*, and *CLE17* are active in a spatially and temporally restricted fashion in the primary root (Fig. 4), whereas the *CLE1*, *CLE5*, *CLE11*, *CLE16*, *CLE17*, and *CLE21* promoters are active in unique subdomains of the developing gynoecium (Fig. 7). No two *CLE* promoters drive expression in identical patterns throughout the plant, and indeed, we observe that even *CLE* genes with very similar sequences have divergent reporter expression patterns. This is exemplified by CLE3 and CLE4, which have an identical CLE motif and pair together in the published phylogenies (Ito et al., 2006; Strabala et al., 2006; Jun et al., 2008; Mitchum et al., 2008). We detect *CLE3* promoter activity in leaf stipules (Fig. 2K) and the pericycle and endodermis of mature roots (Fig. 4, U and V), whereas *CLE4* promoter activity coincides with *CLE3* in the root pericycle (Fig. 4, I and J) but is also found in the hypocotyl pith (Supplemental Fig. S5C), inflorescence branch points (Fig. 5G), stamen filaments (Fig. 6J), and receptacle (Fig. 7O). Thus, while these two genes may function interchangeably in the pericycle, they would appear to have unique activities in the other tissues. The importance of the location of gene expression in conferring functional specificity has also been shown with closely related members of the MADS domain transcription factor family (Pinyopich et al., 2003).

Although many CLE proteins act interchangeably when ectopically expressed in shoots or roots, indicating that tissue distribution is important for their func-

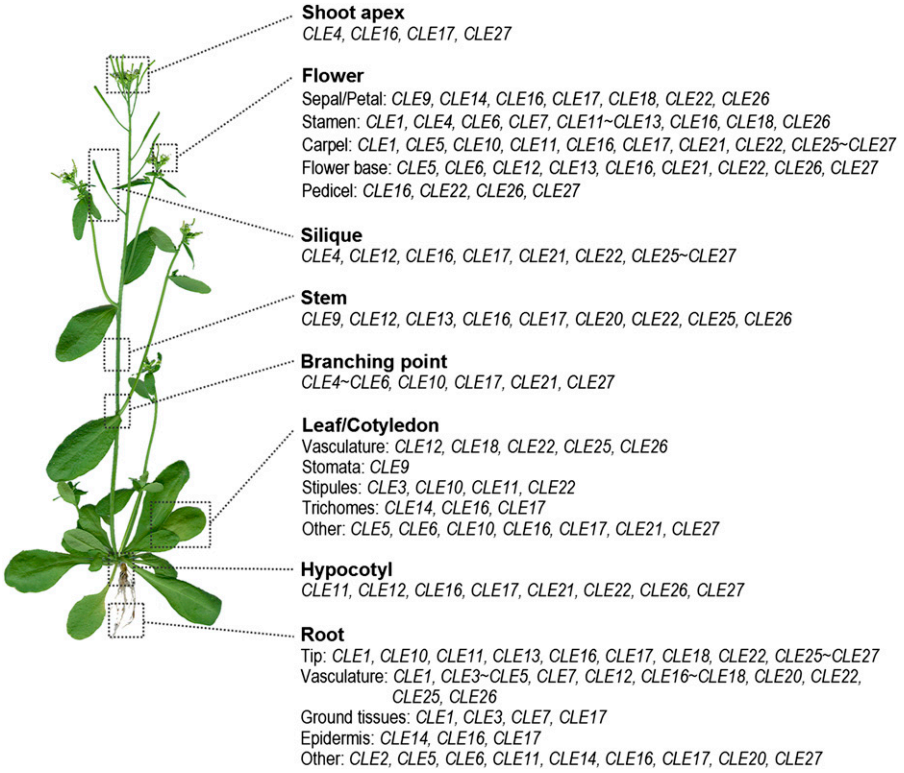

Figure 10. Summary of A-type *CLE* promoter activity in Arabidopsis. Shown is a list of the *CLE* genes expressed in the various tissues of a mature Arabidopsis plant. [See online article for color version of this figure.]

tional specificity, the location of gene expression is not the only determinant of CLE function. Studies have shown that the CLE motif itself determines much of the functional specificity of the proteins in different plant tissues (Fiers et al., 2005, 2006; Ito et al., 2006; Kondo et al., 2006; Ni and Clark, 2006; Meng et al., 2010). We found that the *CLE17* promoter is active in the SAM in a domain that overlaps with *CLV3*, yet its overexpression fails to induce a *CLV3* overexpression SAM termination phenotype (Fig. 8). The CLE peptide of the SAM-expressed *CLE17* gene differs from that of CLV3 at several key residues, including the C-terminal residue (His-12) that plays an essential role in CLV3 peptide function and binding to the CLV1 receptor kinase (Kondo et al., 2008). These data provide an additional piece of evidence that the CLE motif plays a critical role in determining CLE activity and receptor-binding specificity in planta. Other factors contributing to CLE signaling specificity are likely to include the tissue distribution of their cognate receptors as well as of the enzymes that process the CLE proteins to the active arabinosylated peptides (Ohyama et al., 2009).

To date, assessing the biological roles of small signaling peptide gene families has proven to be a significant challenge, primarily due to a lack of hypomorphic or null alleles. These are not available for most CLE family members because the small size of the genes reduces the target size for T-DNA insertion and because the mature molecule consists of only a short stretch of amino acids. We have identified null mutations in the *CLE1*, *CLE7*, *CLE16*, and *CLE18* genes, but in each case the homozygous plants lack detectable morphological phenotypes, indicating that their function may be conditioned by environmental factors and/or masked by redundancy with other CLE peptides. In the future, alternative strategies will be required to specifically target *CLE* genes for down-regulation. Possibilities include artificial microRNAs (Schwab et al., 2006) and increased efficiency homologous recombination (Osakabe et al., 2010; Zhang et al., 2010).

Although each *CLE* promoter is active in a unique spatial and temporal pattern during Arabidopsis development, we observe that multiple *CLE* promoters are active in overlapping patterns within a given tissue. These overlapping *CLE* genes are most likely to have redundant functions; thus, our complete gene family promoter expression analysis serves as a guide to identify potential redundant *CLE* peptides within specific tissues. However, it should be noted that overlapping expression patterns do not necessarily guarantee redundant activities and that *CLE* genes expressed in the same cell types could potentially send opposite signals, as has been observed for members of the EPIDERMAL PATTERNING FACTOR family of small peptide ligands during stomatal development (Abrash and Bergmann, 2010).

Finally, our elucidation of *CLE* promoter activity throughout Arabidopsis development provides a resource for predicting candidate receptors based on their overlapping or neighboring expression patterns. For instance, the *PHLOEM INTERCALATED WITH XYLEM* (*PXY*) gene encodes an LRR receptor kinase that belongs to the same clade of LRR-RLK subclass

XI proteins as CLV1 (Hirakawa et al., 2008). *PXY* is expressed in dividing vascular procambium cells (Fisher and Turner, 2007) and interacts with the B-type CLE peptide CLE41 (Etchells and Turner, 2010). We find that 14 different *CLE* promoters drive GUS activity in the vasculature (Table I). Thus, the products of one or more of these *CLE* genes could act as ligands for PXY and/or for VASCULAR HIGHWAY1, another LRR-RLK expressed in procambial cells throughout the plant (Clay and Nelson, 2002). An LRR-RLK encoded by the *EXCESS MICROSPOROCYTES1/EXTRA SPOROGENOUS CELLS* (*EMS1/EXS*) gene is expressed in the sporogenous and parietal cells of the developing anther, where it controls microsporocyte differentiation and tapetal identity (Canales et al., 2002; Zhao et al., 2002). The *CLE1*, *CLE7*, *CLE12*, *CLE13*, and *CLE25* promoters are all active during early anther formation, making these genes candidates to encode EMS1/EXS ligands. *EMS1/EXS* is also expressed in developing leaf primordia, inflorescence meristems, and young flower buds (Canales et al., 2002). Yet, among the *CLE* promoters active in young anthers, only those of *CLE12*, *CLE13*, and *CLE25* are also active in leaf primordia and none is active in or adjacent to the inflorescence meristem. Thus, broadly expressed receptors such as EMS1/EXS may potentially bind different CLE ligands deriving from different cell types. In conclusion, our systematic analysis of the *CLE* gene family illustrates the complex expression dynamics of these signaling molecules throughout the Arabidopsis life cycle and provides a foundation for identifying and characterizing many ligand-receptor-mediated signaling pathways during plant development.

MATERIALS AND METHODS

Plant Materials

Arabidopsis (*Arabidopsis thaliana*) ecotype Columbia and Landsberg *erecta* plants were used in this study. Seeds were imbibed at 4°C for 3 d before sowing and were grown in a greenhouse under long days (16 h of light and 8 h of dark) with a day/night temperature cycle of 22°C/18°C. Seeds were surface sterilized for 10 min in 5% NaOCl and 0.1% Triton X-100, rinsed in distilled water, and plated on plates containing Murashige and Skoog medium with 0.8% type M agar (Life Technologies), 0.5 mM MES, pH 5.7, 0.5% Suc, and 1 mL/L Gamborg's vitamin solution (Sigma).

Construction of Transgenic Plants

To generate *CLE* promoter:GUS fusion constructs, the 5′ upstream region (974–3,398 bp) of each *CLE* gene was PCR amplified from Columbia genomic DNA and cloned into a binary vector for transformation. For each construct, the binary vector in the *Agrobacterium tumefaciens* strain GV3101 or ASE was introduced into plants by the floral dip method (Clough and Bent, 1998). Primer sequences are listed in Supplemental Table S3.

Histochemical Assays

GUS staining of transgenic plants was performed as described (Jefferson et al., 1987), with the modification that 0.5 mM potassium ferrocyanide and 2.5 mM potassium ferricyanide were used. Incubation times ranged from 2 to 16 h following vacuum infiltration. Subsequent tissue embedding and sectioning were performed as described (Sieburth and Meyerowitz, 1997). For roots and some flower samples, whole-mount clearing was performed in Hoyer's medium (Liu and Meinke, 1998), and the samples were visualized using a Zeiss Axiophot microscope equipped with Nomarski optics. Whole seedlings, inflorescences, and flower specimens were imaged using a Zeiss Stemi 2000-c or a Zeiss Stemi SV11 microscope. GFP fluorescence was visualized using a Leica DM LB fluorescence microscope or a Zeiss LSM 510 confocal microscope with 488-nm/530-nm excitation/emission light.

mRNA Transcript Analysis

cDNA was synthesized from 1 to 5 μg of total RNA using an oligo(dT_{18}) primer and SuperScript III reverse transcriptase (Invitrogen). For RT-PCR, 1 μL of the first-strand cDNA reaction was used as a template. The annealing temperature for RT-PCR was 55°C to 60°C for all primer pairs, and the number of PCR cycles was as follows: *EF1α*, 23 cycles; *TUB4*, 26 cycles; *CLE2*, *CLE16*, *CLE17*, and *CLE27*, 30 cycles; *CLE1*, *CLE3*, *CLE4*, *CLE6*, *CLE7*, and *CLE19*, 35 cycles; *CLE18*, 40 cycles. Primer sequences are listed in Supplemental Table S3.

Supplemental Data

The following materials are available in the online version of this article.

Supplemental Figure S1. *CLE14* and *CLE20* promoter activity in vegetative and reproductive tissues.

Supplemental Figure S2. Examples of *CLE* promoter activity in primary root vasculature.

Supplemental Figure S3. *CLE* promoter activity during lateral root development.

Supplemental Figure S4. *CLE* promoter activity in lateral root tips of 11-d-old-seedlings.

Supplemental Figure S5. *CLE* promoter activity in the shoot apex region.

Supplemental Figure S6. *CLE16*, *CLE17*, and *CLE27* promoter activity in the shoot apex.

Supplemental Figure S7. *CLE8*, *CLE12*, and *CLE22* overexpression phenotypes.

Supplemental Table S1. *CLE* overexpression meristem phenotypes.

Supplemental Table S2. *CLE* insertion alleles.

Supplemental Table S3. Oligonucleotides used in this study.

Supplemental Materials and Methods S1.

ACKNOWLEDGMENTS

We thank Niki Kubat, Vicky Chen, and Liz Fong for assistance handling plants and generating constructs; the RIKEN, SAIL, GABI-KAT, and SALK collections for supplying indexed insertion mutant lines; and Sheila McCormick and Barbara Baker for helpful discussions.

Received July 30, 2010; accepted September 30, 2010; published September 30, 2010.

LITERATURE CITED

Abrash EB, Bergmann DC (2010) Regional specification of stomatal production by the putative ligand CHALLAH. Development **137:** 447–455

Arabidopsis Genome Initiative (2000) Analysis of the genome sequence of the flowering plant Arabidopsis thaliana. Nature **408:** 796–815

Brady SM, Orlando DA, Lee JY, Wang JY, Koch J, Dinneny JR, Mace D, Ohler U, Benfey PN (2007) A high-resolution root spatiotemporal map reveals dominant expression patterns. Science **318:** 801–806

Brand U, Fletcher JC, Hobe M, Meyerowitz EM, Simon R (2000) Dependence of stem cell fate in Arabidopsis on a feedback loop regulated by CLV3 activity. Science **289:** 617–619

Canales C, Bhatt AM, Scott R, Dickinson HG (2002) *EXS*, a putative LRR receptor kinase, regulates male germline cell number and tapetal identity and promotes seed development in Arabidopsis. Curr Biol **12:** 1718–1727

Cartwright DA, Brady SM, Orlando DA, Sturmfels B, Benfey PN (2009) Reconstructing spatiotemporal gene expression data from partial observations. Bioinformatics **25:** 2581–2587

Casamitjana-Martínez E, Hofhuis HF, Xu J, Liu CM, Heidstra R, Scheres B (2003) Root-specific *CLE19* overexpression and the *sol1/2* suppressors implicate a CLV-like pathway in the control of Arabidopsis root meristem maintenance. Curr Biol **13:** 1435–1441

Clark SE, Williams RW, Meyerowitz EM (1997) The *CLAVATA1* gene encodes a putative receptor kinase that controls shoot and floral meristem size in Arabidopsis. Cell **89:** 575–585

Clay NK, Nelson T (2002) VH1, a provascular cell-specific receptor kinase that influences leaf cell patterns in *Arabidopsis*. Plant Cell **14:** 2707–2722

Clough SJ, Bent AF (1998) Floral dip: a simplified method for Agrobacterium-mediated transformation of Arabidopsis thaliana. Plant J **16:** 735–743

Cock JM, McCormick S (2001) A large family of genes that share homology with *CLAVATA3*. Plant Physiol **126:** 939–942

Edgar RC (2004) MUSCLE: multiple sequence alignment with high accuracy and high throughput. Nucleic Acids Res **32:** 1792–1797

Etchells JP, Turner SR (2010) The PXY-CLE41 receptor ligand pair defines a multifunctional pathway that controls the rate and orientation of vascular cell division. Development **137:** 767–774

Fiers M, Golemiec E, van der Schors R, van der Geest L, Li KW, Stiekema WJ, Liu CM (2006) The CLAVATA3/ESR motif of CLAVATA3 is functionally independent from the nonconserved flanking sequences. Plant Physiol **141:** 1284–1292

Fiers M, Golemiec E, Xu J, van der Geest L, Heidstra R, Stiekema W, Liu CM (2005) The 14-amino acid CLV3, CLE19, and CLE40 peptides trigger consumption of the root meristem in *Arabidopsis* through a *CLAVATA2*-dependent pathway. Plant Cell **17:** 2542–2553

Fiers M, Hause G, Boutilier K, Casamitjana-Martínez E, Weijers D, Offringa R, van der Geest L, van Lookeren Campagne M, Liu C-M (2004) Mis-expression of the *CLV3/ESR*-like gene *CLE19* in *Arabidopsis* leads to a consumption of root meristem. Gene **327:** 37–49

Fisher K, Turner S (2007) PXY, a receptor-like kinase essential for maintaining polarity during plant vascular-tissue development. Curr Biol **17:** 1061–1066

Fletcher JC, Brand U, Running MP, Simon R, Meyerowitz EM (1999) Signaling of cell fate decisions by CLAVATA3 in Arabidopsis shoot meristems. Science **283:** 1911–1914

Hirakawa Y, Shinohara H, Kondo Y, Inoue A, Nakanomyo I, Ogawa M, Sawa S, Ohashi-Ito K, Matsubayashi Y, Fukuda H (2008) Non-cell-autonomous control of vascular stem cell fate by a CLE peptide/receptor system. Proc Natl Acad Sci USA **105:** 15208–15213

Hobe M, Müller R, Grünewald M, Brand U, Simon R (2003) Loss of CLE40, a protein functionally equivalent to the stem cell restricting signal CLV3, enhances root waving in Arabidopsis. Dev Genes Evol **213:** 371–381

Ito Y, Nakanomyo I, Motose H, Iwamoto K, Sawa S, Dohmae N, Fukuda H (2006) Dodeca-CLE peptides as suppressors of plant stem cell differentiation. Science **313:** 842–845

Jefferson RA, Kavanagh TA, Bevan MW (1987) GUS fusions: beta-glucuronidase as a sensitive and versatile gene fusion marker in higher plants. EMBO J **6:** 3901–3907

Jeong S, Trotochaud AE, Clark SE (1999) The *Arabidopsis CLAVATA2* gene encodes a receptor-like protein required for the stability of the CLAVATA1 receptor-like kinase. Plant Cell **11:** 1925–1934

Jun JH, Fiume E, Fletcher JC (2008) The CLE family of plant polypeptide signaling molecules. Cell Mol Life Sci **65:** 743–755

Kondo T, Nakamura T, Yokomine K, Sakagami Y (2008) Dual assay for MCLV3 activity reveals structure-activity relationship of CLE peptides. Biochem Biophys Res Commun **377:** 312–316

Kondo T, Sawa S, Kinoshita A, Mizuno S, Kakimoto T, Fukuda H, Sakagami Y (2006) A plant peptide encoded by CLV3 identified by in situ MALDI-TOF MS analysis. Science **313:** 845–848

Laux T, Mayer KFX, Berger J, Jürgens G (1996) The WUSCHEL gene is required for shoot and floral meristem integrity in Arabidopsis. Development **122:** 87–96

Liu CM, Meinke DW (1998) The titan mutants of Arabidopsis are disrupted in mitosis and cell cycle control during seed development. Plant J **16:** 21–31

Meng L, Ruth KC, Fletcher JC, Feldman L (2010) The roles of different CLE domains in *Arabidopsis* CLE polypeptide activity and functional specificity. Mol Plant **3:** 760–772

Mitchum MG, Wang X, Davis EL (2008) Diverse and conserved roles of CLE peptides. Curr Opin Plant Biol **11:** 75–81

Müller R, Bleckmann A, Simon R (2008) The receptor kinase CORYNE of *Arabidopsis* transmits the stem cell-limiting signal CLAVATA3 independently of CLAVATA1. Plant Cell **20:** 934–946

Ni J, Clark SE (2006) Evidence for functional conservation, sufficiency, and proteolytic processing of the CLAVATA3 CLE domain. Plant Physiol **140:** 726–733

Ogawa M, Shinohara H, Sakagami Y, Matsubayashi Y (2008) Arabidopsis CLV3 peptide directly binds CLV1 ectodomain. Science **319:** 294

Ohyama K, Shinohara H, Ogawa-Ohnishi M, Matsubayashi Y (2009) A glycopeptide regulating stem cell fate in *Arabidopsis thaliana*. Nat Chem Biol **5:** 578–580

Osakabe K, Osakabe Y, Toki S (2010) Site-directed mutagenesis in *Arabidopsis* using custom-designed zinc finger nucleases. Proc Natl Acad Sci USA **107:** 12034–12039

Pinyopich A, Ditta GS, Savidge B, Liljegren SJ, Baumann E, Wisman E, Yanofsky MF (2003) Assessing the redundancy of MADS-box genes during carpel and ovule development. Nature **424:** 85–88

Rojo E, Sharma VK, Kovaleva V, Raikhel NV, Fletcher JC (2002) CLV3 is localized to the extracellular space, where it activates the *Arabidopsis* CLAVATA stem cell signaling pathway. Plant Cell **14:** 969–977

Schoof H, Lenhard M, Haecker A, Mayer KFX, Jürgens G, Laux T (2000) The stem cell population of Arabidopsis shoot meristems is maintained by a regulatory loop between the CLAVATA and WUSCHEL genes. Cell **100:** 635–644

Schwab R, Ossowski S, Riester M, Warthmann N, Weigel D (2006) Highly specific gene silencing by artificial microRNAs in *Arabidopsis*. Plant Cell **18:** 1121–1133

Sharma VK, Ramirez J, Fletcher JC (2003) The Arabidopsis CLV3-like (CLE) genes are expressed in diverse tissues and encode secreted proteins. Plant Mol Biol **51:** 415–425

Shiu SH, Bleecker AB (2001) Receptor-like kinases from Arabidopsis form a monophyletic gene family related to animal receptor kinases. Proc Natl Acad Sci USA **98:** 10763–10768

Sieburth LE, Meyerowitz EM (1997) Molecular dissection of the AGAMOUS control region shows that cis elements for spatial regulation are located intragenically. Plant Cell **9:** 355–365

Stahl Y, Wink RH, Ingram GC, Simon R (2009) A signaling module controlling the stem cell niche in Arabidopsis root meristems. Curr Biol **19:** 909–914

Strabala TJ, O'Donnell PJ, Smit AM, Ampomah-Dwamena C, Martin EJ, Netzler N, Nieuwenhuizen NJ, Quinn BD, Foote HCC, Hudson KR (2006) Gain-of-function phenotypes of many CLAVATA3/ESR genes, including four new family members, correlate with tandem variations in the conserved CLAVATA3/ESR domain. Plant Physiol **140:** 1331–1344

Whitford R, Fernandez A, De Groodt R, Ortega E, Hilson P (2008) Plant CLE peptides from two distinct functional classes synergistically induce division of vascular cells. Proc Natl Acad Sci USA **105:** 18625–18630

Yadav RK, Girke T, Pasala S, Xie M, Reddy GV (2009) Gene expression map of the Arabidopsis shoot apical meristem stem cell niche. Proc Natl Acad Sci USA **106:** 4941–4946

Zhang F, Maeder ML, Unger-Wallace E, Hoshaw JP, Reyon D, Christian M, Li X, Pierick CJ, Dobbs D, Peterson T, et al (2010) High frequency targeted mutagenesis in *Arabidopsis thaliana* using zinc finger nucleases. Proc Natl Acad Sci USA **107:** 12028–12033

Zhao DZ, Wang GF, Speal B, Ma H (2002) The excess microsporocytes1 gene encodes a putative leucine-rich repeat receptor protein kinase that controls somatic and reproductive cell fates in the Arabidopsis anther. Genes Dev **16:** 2021–2031